NAPHTHYRIDINOMYCIN-DNA ADDUCTS: A MOLECULAR MODELING STUDY

M. B. Cox†, P. Arjunan and S. K. Arora*

Department of Crystallography and Pittsburgh Cancer Institute, University of Pittsburgh, Pittsburgh, PA 15260, U.S.A.

(Received for publication November 16, 1990)

Monocovalent groove binding complexes of antitumor antibiotic naphthyridinomycin and its analogs with DNA sequence $d(ATGCAT)_2$ have been studied by molecular mechanics to understand which enantiomer of the drug and what chirality at C(7) of the drug are preferred for forming better drug-DNA adducts. The effect of hydroquinone intermediate and the substitution at C(11) on drug-DNA interactions have also been investigated. The results indicate that the enantiomer that forms the best adduct is different from the one reported earlier in the literature. The drug with an *R* configuration at C(7) is preferred for binding. The hydroquinone models do not necessarily provide a given analog of the drug with additional favorable DNA interactions. The substitution at C(11) by OH provides the best binding model. This finding agrees well with the results from previous biochemical studies. The sequence specific studies indicate that the sequence $d(ATGCAT)_2$ is slightly preferred over others.

Naphthyridinomycin (NP) and its cyano derivative cyanonaphthyridinomycin shown in Fig. 1, are heterocyclic antibiotics produced from culture filtrates of *Streptomyces lusitanus*[1]. These antibiotics contain complicated and unusual structure that contain three basic nitrogens. They are potent both as an antimicrobial and as an antitumor agent. Several experiments have indicated that the mode of action of this family of antibiotics involves the inhibition of DNA synthesis, which results in unbalanced cell growth[2]. It has also been shown that NP inhibits the enzyme DNA-dependent RNA polymerase *in vitro*. The binding of NP to DNA is increased in the presence of reducing agent, such as dithiothreitol. This may be due to the conversion of quinone moiety into a hydroquinone moiety. The studies on binding of the antibiotic to DNA[3,4], have suggested that the bond between the NP molecule and DNA is very strong and probably covalent. NP binds very strongly to [poly(dG)·poly(dC)] sequences. The exact mechanism of binding of the naphthyridinomycins to DNA is not known but has been suggested[4] to be similar to other carbinolamine-containing antibiotics such as pyrrolo[1,4]benzodiazepine antibiotics which covalently bind to the N2 of the guanine in the minor groove of the DNA[5].

The role of the functional group at C(11) has been studied[6] and it has been shown that conversion

Fig. 1. Chemical structures of naphthyridinomycins.

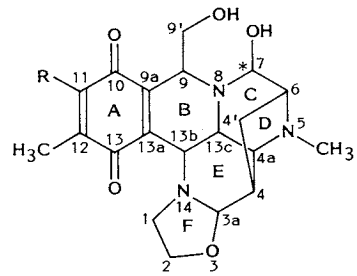

NP	$R=OCH_3$
NPA	$R=NH_2$
NPAHY	$R=NH_2$ and OH at C_{10} and C_{13}
NPH	$R=OH$
NPHHY	$R=OH$ and OH at C_{10} and C_{13}
NPHY	$R=OCH_3$ and OH at C_{10} and C_{13}

† Present address: Vista Chemical Co., Austin, TX 78720, U.S.A.

of the methoxyl group at C(11) to a hydroxyl group increases the activity of NP both as an antimicrobial and as an antitumor agent. Similarly, conversion of the methoxyl group to an amine group confers greater antimicrobial activity on the drug without increasing its antitumor potential to a great extent[7]. The question is whether or not these alterations in the substituent at C(11) affect the drug-DNA interactions at the binding site, and if so, do these effects play a role in the differences observed in biological activity among the various derivatives.

Molecular modeling in conjunction with molecular mechanical calculations can be a powerful tool to probe structures of molecules and complexes in three dimensions. Theoretical studies on the interaction of benzodiazepine antibiotics with DNA have also been carried out recently[8~10]. The crystal structures of NP and its cyano derivative are known[11,12]. Modeling studies were undertaken in an attempt to understand the interactions between DNA and the naphthyridinomycins upon the formation of the adduct. These included studies designed to determine: 1) whether the drug was a true groove binder or a partial intercalator, 2) which enantiomer of the drug produced the best DNA adduct model, 3) what was the preferred chirality of C(7) at the binding site, 4) what role the hydroquinone form of the drug played in DNA interactions and 5) how substituent changes at C(11) affected drug-DNA interactions. The first question was answered by our previous modeling studies[12] with $d(ATGCAT)_2$, indicating that groove binding was preferable to partial intercalation. The structure used in that study was determined crystallographically. The crystallographic studies had provided only the relative stereochemistry of the active enantiomer, but not its absolute stereochemistry. Thus, it was indeterminate which enantiomer of NP was examined by crystallography. From their synthetic studies, EVANS *et al.*[13] revealed that the stereochemistry reported in the literature was not correct and the structure should be reversed. The absolute stereochemistry of the drug becomes important when considering how the drug interacts with the chiral DNA molecule. Furthermore, since DNA binding occurred at a chiral carbon on the drug, it was important to determine whether binding in the *R* configuration or in the *S* configuration at C(7) provided the better model. In this study we have addressed questions two through five.

Materials and Methods

Conformational studies were carried out by molecular mechanics method using the program MACROMODEL (version 2.0 and 2.5). The crystal structure of NP[11] was used as the initial structure in this investigation. The drug and its analogs were energy minimized using the AMBER force field parameters of WEINER *et al.*[14]. The cut off distance for non bonded pairs was 99 Å. The hexanucleotide duplex structure $d(ATGCAT)_2$ was constructed in the B form and energy minimized. The drug-DNA adduct models were built from the energy-minimized structures of the drug and B-DNA. The parent drug (NP) and its analogs were visually docked near the binding site (2-amino group of guanine) in the minor groove of DNA using an EVANS and SUTHERLAND

Fig. 2. Schematic illustration of $d(ATGCAT)_2$.

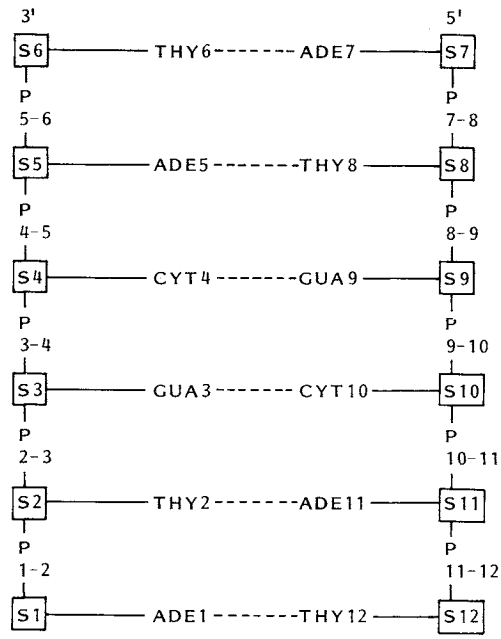

390 graphics system. Translational and rotational simplex searches helped to eliminate unfavorable steric contacts. The drug was then covalently bound to the N2 of the GUA9 (Fig. 2) residue. The adducts were minimized using the AMBER force field[14] and a conjugate gradient minimization using the Perry self-correcting first- derivative method with restarts. Contributions of hydrogen bonds were taken into account. All minimizations of drugs, DNA and adducts were carried out to a RMS first derivative of 0.1 Kj/A. A distance-dependent dielectric constant $\varepsilon > Rij$ was used in all the calculations.

Results and Discussion

The DNA sequence $d(ATGCAT)_2$ was used in the chirality and analog modeling studies and is shown schematically in Fig. 2. This sequence was chosen because it provided a unique binding site for the drug at the guanine residue, and also other covalently binding drugs had been studied with this sequence.

To investigate which enantiomer of NP provided the better adduct model, and what is the preferred chirality of binding, four adduct models were constructed containing the two enantiomers of NP, each bound in a different configuration. The results of the minimization of each adduct are listed in Table 1. NPR and NPS are adducts derived from the enantiomer (reported in crystallographic studies) bound to the DNA in the *R* and *S* configurations, respectively. NPER and NPES refer to the adducts derived from the other enantiomer (EVANS) which was generated from the crystal structure by multiplying the fractional coordinate y/b by (−1.0) for every atom in NP. Analysis of the energetics of the four models indicates that the drug with the *R* configuration at C(7) forms a better adduct than the drug with *S* configuration for both enantiomers. The net binding energies are compared. The energy differences are of the order of 3 to 7 Kcal. The best adduct model among all four models is the NPER (EVANS enantiomer and *R* configuration at C7) with a value of −9.4 Kcal. The DNA distortion energies also indicate that the *R* configuration of the drug distorts the DNA the least. The DNA distortion energy for the NPES model is much higher than for the other three models. Similar differences in DNA distortion energies were observed in other antibiotic-DNA adducts studies[8,9].

Fig. 3 shows the NPER model. Some quantified characteristics of the NPER model are given in

Table 1. Energy data (in Kcal) using MACROMODEL 2.0 for NP and $d(ATGCAT)_2$ models.

Complex	Total[a]	Drug[b] (add.)	DNA[c] (add.)	Drug[d] distort	DNA[e] distort	Intermol.[f] interact.	Net[g] binding
NPS	−408.50	53.91	−444.23	7.51	12.96	−18.18	2.29
NPR	−414.76	51.49	−445.23	5.09	11.96	−21.02	−3.97
NPES	−403.84	48.44	−423.81	2.04	33.38	−28.47	6.95
NPER	−420.18	47.34	−439.51	0.94	17.68	−28.01	−9.39
NPHY	−418.85	45.91	−438.32	1.08	18.87	−26.44	−6.49
NPA	−419.42	47.17	−441.81	1.75	15.38	−24.78	−7.65
NPAHY	−422.52	43.69	−437.87	4.44	19.32	−28.34	−4.53
NPH	−427.69	49.00	−444.77	2.96	12.42	−31.92	−16.54
NPHHY	−415.56	39.92	−437.99	−0.25	19.20	−17.49	1.46

Minimized energy values for free NP, NPA, NPH, NPHY, NPAHY, NPHHY and $d(ATGCAT)_2$ are 46.40, 45.42, 46.04, 44.83, 38.25, 40.17 and −457.19 Kcal, respectively.

[a] The total energy is the energy calculated for the entire adduct.

[b,c] Drug and DNA energies after separating from the minimized adduct.

[d,e] These are calculated by subtracting the intramolecular energies of the drug and DNA in the complex from their energies obtained by separately minimizing each isolated molecule.

[f] Intermolecular interaction energy is the total energy minus the separate drug and DNA energies.

[g] Net binding energy is the intermolecular interaction energy plus the drug and DNA distortion energies.

Fig. 3. Stereopair of energy minimized model NPER.

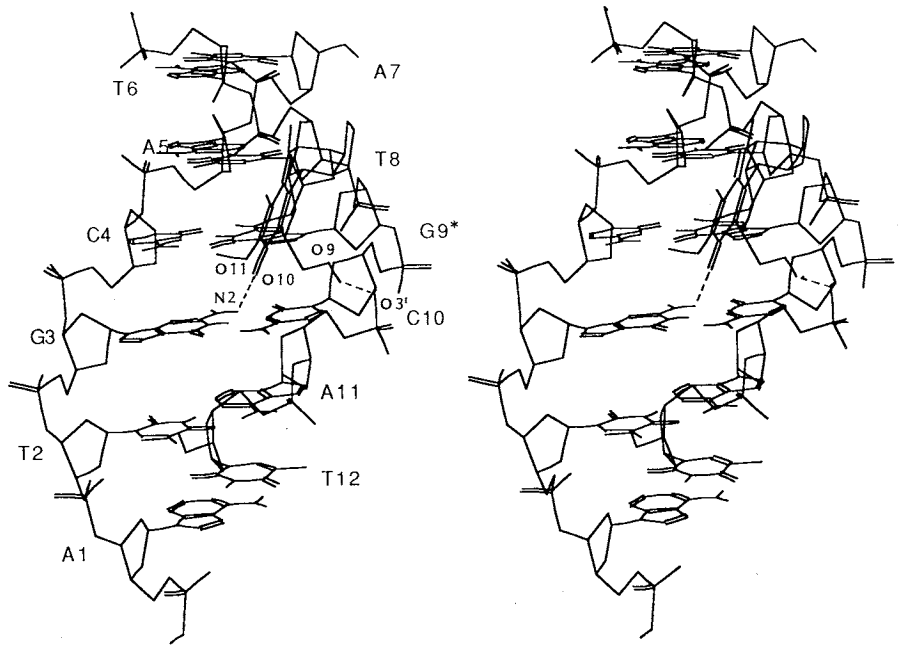

Table 2. Hydrogen bonds in NP/d(ATGCAT)$_2$ models.

Complex	Bond (donor-acceptor)	Distance (Å)	Angle (deg)	Complex	Bond (donor-acceptor)	Distance (Å)	Angle (deg)
NPS	O(9)-O(2) [CYT4]	2.761	138.0	NPA	O(9)-O(3') [CYT10]	2.784	170.9
	N(2) [GUA3]-O(10)	2.764	144.7		N(2) [GUA3]-O(10)	2.750	141.2
NPR	O(9)-O(1') [CYT4]	2.805	158.5	NPAHY	O(9)-O(3') [CYT10]	2.769	173.1
	N(2) [GUA3]-O(10)	2.930	120.4		O(10)-O(1') [ADE11]	2.813	146.5
NPES	O(9)-O(1') [ADE11]	2.756	147.5		O(13)-OP [THY6]	2.597	161.2
	N(2) [GUA3]-O(10)	2.889	152.1	NPH	O(9)-O(3') [CYT10]	2.766	169.4
NPER	O(9)-O(3') [CYT10]	2.798	171.4		N(2) [GUA3]-O(10)	2.795	139.5
	N(2) [GUA3]-O(10)	2.730	140.0		O(11)-O(3') [CYT4]	2.747	151.5
NPHY	O(9)-O(3') [CYT10]	2.809	163.6	NPHHY	O(9)-O(3') [CYT10]	2.785	166.8
	N(2) [GUA3]-O(10)	2.751	150.3		O(13)-OP [THY6]	2.597	161.1
	O(10)-O(11)	2.659	118.2		O(10)-O(11)	2.624	119.2
	O(13)-OP [THY6]	2.595	166.8				

Tables 2 and 3. Table 2 lists the hydrogen bonds formed in this model. The hydrogen bonds include a bond between O(9) of the drug and O(2) of CYT4, and a bond between O(10) of the drug and N(2) of GUA3. Data on the conformational properties of the DNA in the NPER adduct are given in Table 3, and are compared with those of minimized d(ATGCAT)$_2$. The glycosidic angles of the nucleotides all stay in an *anti* conformation in the NPER model. The nucleotide which shows the highest glycosidic angle deviation from the minimized DNA model is CYT10. This is also the nucleotide directly below the binding site at GUA9. The glycosidic angle of CYT10 undoubtedly changes to sterically accommodate the NP molecule. The sugars of the strand to which the drug is bound retain the same conformations as seen in the minimized-DNA model, as measured by the angle of pseudorotation, P[15]. Except for the sugar of ADE1, the sugars of the strand opposite of the binding site all deviate in conformation. All sugars in both strands

Table 3. P and Tm values for the sugars in the minimized NPER and d(ATGCAT)$_2$ models.

Residue	NPER model			ATGCAT model		
	P	Tm	X	P	Tm	X
ADE1	185.49	32.95	−101.20	185.82	32.67	−102.40
THY2	113.99	40.33	−126.00	133.19	42.52	−115.40
GUA3	148.33	40.66	−125.10	179.78	33.30	−123.10
CYT4	176.51	34.16	−117.20	154.93	39.19	−115.00
ADE5	144.08	41.98	−116.10	178.95	32.01	−120.00
THY6	175.77	34.39	−102.80	146.78	38.85	−117.70
ADE7	185.82	32.67	−102.70	185.82	32.67	−102.40
THY8	135.55	43.29	−109.20	133.19	42.52	−115.20
GUA9	185.87	33.98	−128.20	179.83	33.30	−123.10
CYT10	154.81	42.21	− 91.60	154.80	39.23	−114.80
ADE11	189.99	31.27	−129.60	179.01	32.00	−120.00
THY12	147.38	39.18	−121.60	146.74	38.87	−117.70

fall in the region between the pure C3′-exo (P = 198°) and pure 1′-exo (P = 126°) conformations, the center of which is the C2′-endo conformation (P = 162°) which is seen in B DNA. None of the sugars adopt a C3′-endo conformation. In fact, for the sugars of the strand opposite the binding site which show the most deviation, P decreases for only three of these sugars, as would be seen in a shift from a C2′-endo to a C3′-endo conformation, but actually increases for the other two. Thus, there does not seem to be a general shift to the A DNA conformation which would prefer C3′-endo sugars with P values in the region of 0° to 36°. Rather, the deviations in sugar pucker are minor adjustments which relieve steric stress in the complex, but the sugars tend to remain in the B conformation.

Several analog models were built based on NPER (the preferred binder, reffered to as NP ahead) to allow us to investigate the roles that reduction of the quinone ring to a hydroquinone and substituent changes at C(11) might play in DNA binding. NPHY was built from the preminimized NPER model. It contains the parent NP molecule with the quinone ring converted to a hydroquinone. NPA was also built from the preminimized NPER model. It contains the quinone form of the parent NP molecule with the methoxyl at C(11) converted to a primary amine. NPAHY is the hydroquinone form of the NPA model. Finally, NPH was built from the preminimized NPER model and represents the C(11) hydroxyl derivative of the parent NP molecule. NPHHY is the hydroquinone form of NPH. The results of the minimizations of these models are given in Table 1 and the intermolecular hydrogen bonds found in all the models are listed in Table 2.

An examination of the various hydroquinone models yields interesting results. The hydrogen bonding pattern involving O(9) is the same in these models as is seen in the NPER model. There is an O(9) to O(3′) of the CYT10 hydrogen bond with distances of 2.81, 2.77, and 2.78 Å for NPHY, NPAHY, and NPHHY, respectively, compared with a distance of 2.78 Å seen in NPER. An additional hydrogen bond is also predicted in all three hydroquinone models involving O(13) of the hydroquinone and a phosphate oxygen of THY6. The distances of this hydrogen bond are 2.59, 2.60, and 2.62 Å for NPHY, NPAHY, and NPHHY, respectively. The hydrogen bonding pattern involving O(10), however, varies significantly in these models. In NPHY, the same N(2) of GUA3 to O(10) hydrogen bond seen in the NPER model is observed with a distance of 2.75 Å. In NPAHY, the hydrogen bond involving O(10) is to O(1′) of ADE11 with a distance of 2.81 Å. In NPHHY, no hydrogen bonding involving O(10) is seen. Instead, the O(10)

proton is oriented toward the hydroxyl substituent at C(11). The distance between O(10) and O(11) is 2.62 Å, which is correct for an intramolecular hydrogen bond. It is interesting to note that the C(11) hydroxyl in the NPHHY model does not hydrogen bond to the DNA either. Therefore the intramolecular hydrogen bond between the hydroxyl at C(11) and O(10) interferes with any potential that either hydroxyl may have for DNA interaction.

Despite the additional hydrogen bond between the DNA backbone and O(13), the hydroquinone analogs are not lower in energy with respect to their analogous quinone forms. In fact, NPHHY provides the highest net binding energy model of all the NPER analog models. This is primarily due to the fact that its intermolecular interaction energy is significantly higher than that of the other models. This, in turn, can be directly related back to the lack of hydrogen bonding involving the DNA and either O(10) or O(11) in this model. These observations tend to suggest that formation of a hydroquinone upon reductive activation does not necessarily provide a given analog of the drug with additional favorable DNA interactions. Rather, the data obtained in these modeling experiments tend to support the hypothesis that the major activation mechanism involves the conversion of C(7) into an sp^2 carbon to promote reactivity. Even if this is the case, the formation of the hydroquinone still undoubtedly affects DNA binding interactions *via* altering hydrogen bonding patterns, though not as a major activation mechanism. It is important to temper these conclusions, however, by noting that the results obtained by these experiments may be highly dependent on the specific DNA sequence chosen for the models. Further modeling studies on alterations in the DNA sequence and their effects upon drug analog binding are in progress.

As to the effects of substitution at C(11) on DNA binding, the experiments provided mixed results. It is important to note that the hydrogen bonding characteristics of the models differ from those seen in the preliminary models previously discussed. This is, of course because the second round of modeling studies led to revision of the enantiomer and configuration of binding used in the models. It is still the goal of this study, however, to see if the derivative models provide lower energy models than the parent compound, and whether the C(11) amine and hydroxyl substituents of these derivatives are involved in hydrogen bonding with the DNA. In both NPA and NPH, the hydrogen bonding pattern involving both O(9) and O(10) is the same as that seen in the parent compound model NPER. The O(9) to O(3′) of CYT10 bonds have distances of 2.78 and 2.77 Å in NPA and NPH, compared with 2.80 Å in NPER. The N(2) of GUA3 to O(10) bonds have distances of 2.75 and 2.79 Å for NPA and NPH, respectively, compared with a distance of 2.73 Å seen in NPER. The C(11) hydroxyl in NPH is involved in an additional hydrogen bond with the DNA. An O(11) to O(3′) of CYT4 bond has a distance of 2.75 Å. The C(11) primary amine in NPA is not involved in any hydrogen bonding with the DNA.

The hydroxyl analog model, NPH (Fig. 4), is the lowest energy model of the three quinone models in terms of both total energy, and in terms of net binding energy. This is perhaps partially due to the additional hydrogen bonding with the DNA provided by the C(11) hydroxyl moiety. The models arranged in order of increasing net binding energy are: NPH < NPER < NPA. Note that the amine derivative model has the highest energy. The model NPA shows no additional DNA hydrogen bonding not seen in the methoxyl derivative model NPER. However, the hydroquinone models arranged in order of increasing net binding energy are: NPHY < NPAHY < NPHHY. All six models arranged in order of increasing net binding energy are: NPH < NPER < NPA < NPHY < NPAHY < NPHHY.

Perhaps the hydroxyl derivative is more biologically active than the parent compound because its quinone derivative forms the lowest energy DNA adduct than either the quinone or the hydroquinone

Fig. 4. Stereopair of NPH-d(ATGCAT)$_2$ energy minimized model.

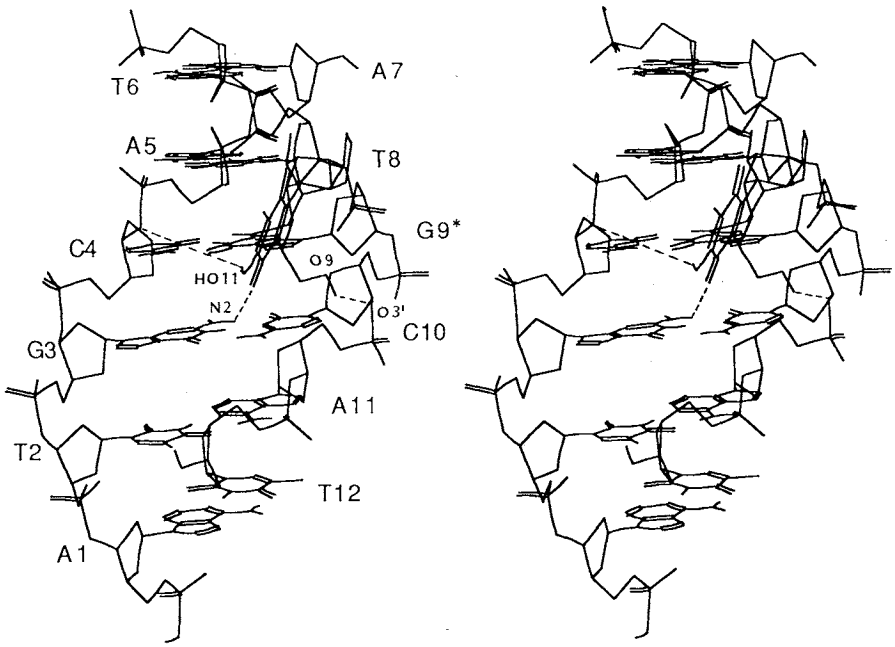

form of the parent compound. This may provide the hydroxyl derivative a binding advantage, even though its hydroquinone derivative forms such a high-energy adduct with DNA. Perhaps the amine derivative is biologically more active because both its quinone and hydroquinone variations can form lower energy DNA adducts than the hydroquinone form of the parent compound. This may provide the amine derivative with a binding advantage even though the parent compound forms a lower energy DNA adduct in its quinone form. While hydrogen bonding does play a role in explaining the activity of the hydroxyl derivative, the activity of the amine derivative may be more related to the overall electronic distribution changes across the molecule caused by an amine for a methoxyl substitution.

Sequence Specifity

In order to understand whether the binding of the naphthyridinomycin with DNA is sequence dependent, we carried out studies on the complexes of naphthyridinomycin and its hydroxyl analog NPH with different sequences of DNA. We changed the bases at the 3′ and 5′ end of guanine (G9) to which the drug is covalently bound with the corresponding WATSON-CRICK base partner on the complementary strands in the hexamer. Thus sixteen oligodeoxynucleotides [AGG*GAT*, AAG*GAT, AGG*AAT, AAG*AAT, ACG*GAT, ATG*GAT, ACG*AAT, ATG*AAT, AGG*CAT, AGG*TAT, AAG*CAT, AAG*TAT, ACG*CAT, ACG*TAT, ATG*CAT, ATG*TAT] adduct with NP and NPH were studied.

Table 4 gives the energetics of complexes of NP with DNA sequences mentioned above. As previously discussed the effect of the drug on binding to different sequence of DNA can be deduced in term of net binding energy or DNA distortion energy. Based on net binding energy the preferred sequence are ATGCAT, AGGCAT and AGGGAT while based on DNA distortion energy the preferred sequence are ATGCAT, AAGCAT and AGGCAT. These three sequence are with in 1.5 Kcal of each other but stand out from the other. The sequence ATGCAT is preferred over the others both in net binding energy and helix

Table 4. Energy minimization results of NP-DNA sequence specificity study.

Sequence	Total[a]	DNA[c] (add.)	Drug[b] (add.)	DNA	Drug[d] distort	DNA[e] distort	Intermol.[f] int.	Net[g] binding
AGGGAT	−625.6	−634.4	50.2	−648.4	3.8	14.0	−41.4	−23.6
AAGGAT	−642.7	−625.3	49.6	−667.8	3.2	15.5	−40.1	−21.4
AGGAAT	−640.3	−654.2	48.9	−670.7	2.5	16.5	−35.1	−16.1
AAGAAT	−657.4	−671.8	48.6	−690.0	2.2	18.2	−34.2	−13.8
ACGGAT	−606.1	−613.9	49.1	−650.5	2.7	36.6	−41.2	− 1.9
ATGGAT	−638.5	−648.7	48.7	−669.3	2.3	20.6	−38.5	−15.6
ACGAAT	−622.8	−636.3	48.3	−679.1	0.1	42.7	−34.8	7.9
ATGAAT	−656.4	−671.4	48.2	−683.9	1.8	12.6	−33.2	−18.8
AGGCAT	−624.3	−635.1	48.8	−646.7	2.4	11.6	−38.1	−24.1
AGGTAT	−637.8	−651.1	48.8	−663.0	2.4	11.9	−35.5	−21.1
AAGCAT	−641.5	−655.4	48.9	−666.7	2.5	11.3	−35.1	−21.3
AAGTAT	−653.9	−667.7	47.8	−687.9	1.4	20.2	−34.1	−12.5
ACGCAT	−607.2	−618.6	48.7	−653.1	2.3	34.5	−37.3	− 0.5
ACGTAT	−619.9	−633.8	48.9	−667.9	2.5	34.2	−35.1	1.6
ATGCAT	−641.5	−653.4	48.5	−663.7	2.1	10.3	−36.6	−24.2
ATGTAT	−654.6	−669.2	48.9	−686.3	2.5	17.2	−34.3	−14.6

These energy minimization were carried out with MACROMODEL version 2.5.
[a~g] See a footnote in Table 1.

Table 5. Hydrogen bond parameters involving NP- oligodeoxynucleotides in the covalent complexes. The drug is bound to GUA9 of complementary strand.

Sequence	Donor	Acceptor	Distance (Å)	Angle (°)
$A_1G_2G_3G_4A_5T_6$	O9′ (NP)	O3′ (GUA10)	2.770	167.2
	N2 (GUA10)	O10 (NP)	2.879	168.5
AAGGAT	O9′ (NP)	O3′ (GUA10)	2.772	167.2
	N2 (GUA10)	O10 (NP)	2.870	168.1
AGGAAT	O9′ (NP)	O3′ (ADE10)	2.744	157.8
AAGAAT	O9′ (NP)	O3′ (ADE10)	2.755	160.1
ACGGAT	O9′ (NP)	O3′ (GUA10)	2.766	166.5
	N2 (GUA10)	O10 (NP)	2.866	171.7
ATGGAT	O9′ (NP)	O3′ (GUA10)	2.769	167.3
	N2 (GUA10)	O10 (NP)	2.853	169.2
ACGAAT	O9′ (NP)	O3′ (ADE10)	2.763	162.9
ATGAAT	O9′ (NP)	O3′ (ADE10)	2.761	163.6
AGGCAT	O9′ (NP)	O3′ (CYT10)	2.790	169.7
	N2′ (GUA3)	O10 (NP)	2.748	137.6
AGGTAT	O9′ (NP)	O3′ (THY10)	2.783	168.0
AAGCAT	O9′ (NP)	O3′ (CYT10)	2.783	168.8
	N2 (ADE3)	O10 (NP)	2.752	137.8
AAGTAT	O9′ (NP)	O3′ (THY10)	2.782	165.0
ACGCAT	O9′ (NP)	O3′ (CYT10)	2.785	170.0
	N2 (CYT3)	O10 (NP)	2.743	137.3
ACGTAT	O9′ (NP)	O3′ (THY10)	2.778	167.6
ATGCAT	O9′ (NP)	O3′ (CYT10)	2.787	169.5
	N2 (THY3)	O10 (NP)	2.739	137.7
ATGTAT	O9′ (NP)	O3′ (THY10)	2.779	167.0

distortion energy but not by much. In case of naphthyridinomycin no experimental data such as footprinting is available to indicate preferrence for a certain sequence. Table 5 gives the hydrogen bond distances observed in different complexes. One feature that standsout from this table is that whenever the base in position 10 (Fig. 2) is A or T, there is decrease in hydrogen bonding.

Table 6. Energies of sequence specific study of NPH with DNA.

Sequence	Total[a]	DNA[c] (add.)	Drug[b] (add.)	DNA	Drug[d] distort	DNA[e] distort	Intermol.[f] int.	Net[g] binding
AGGGAT	−627.9	−633.0	51.4	−648.4	5.4	15.4	−46.3	−25.5
AAGGAT	−642.1	651.4	48.7	−667.8	2.7	16.4	−39.4	−20.1
AGGAAT	−639.4	−650.0	51.0	−670.7	5.0	20.7	−40.4	−14.7
AAGAAT	−663.1	−666.6	49.8	−690.0	3.8	23.4	−46.3	−19.1
ACGGAT	−611.7	−616.2	51.6	−605.5	5.6	34.3	−47.1	− 7.2
ATGGAT	−639.1	−654.4	51.4	−669.3	5.4	14.9	−36.1	−15.8
ACGAAT	−622.7	−633.5	51.6	−769.1	5.6	45.6	−40.8	10.4
ATGAAT	−654.5	−668.6	49.5	−688.9	3.5	20.3	−35.4	−11.6
AGGCAT	−625.9	−632.9	51.4	−646.7	5.4	13.8	−44.4	−25.2
AGGTAT	−639.3	−651.8	50.9	−663.0	4.9	11.2	−38.4	−22.3
AAGCAT	−608.7	−653.5	50.3	−666.7	4.3	13.2	− 5.6	11.9
AAGTAT	−661.2	−659.8	50.2	−687.9	4.2	28.1	−51.6	−19.9
ACGCAT	−608.9	−617.4	52.4	−653.1	6.4	35.7	−43.9	− 1.8
ACGTAT	−619.6	−632.5	52.0	−668.0	6.0	35.5	−39.1	2.4
ATGCAT	−644.6	−654.2	52.1	−663.7	6.1	9.5	−42.5	−26.9
ATGTAT	−653.9	−668.4	49.8	−686.4	3.8	18.0	−35.3	−13.5

[a~g] See a footnote in Table 1.

Table 6 gives the energy minimization results on complexes of NPH with DNA. Here again, based on both net binding energy and DNA distortion energy, the sequence ATGCAT comes out ahead. The next two base on DNA distortion energy are AGGTAT and AAGCAT while based on net binding energy AGGGAT and AGGCAT follow.

A few notes of caution are (1) that since solvent and counter ion effects have not been taken in to account, the molecular mechanics approach cannot provide quantitative results. But since this study has been done with closely related analogs of naphthyridinomycins, the comparison of net binding energies can be useful in studying the interaction of this drug with DNA. (2) These studies yield no information on reactivity, dealing only with energies and conformation of adducts after the reaction.

Supplementary Material

Tables of partial atomic charges for the drug and its analogs.

Acknowledgments

The financial support of this research by National Institutes of Health (GM32690) is greatly appreciated. The authors would also like to thank Dr. W. C. STILL of Columbia University for providing the MACROMODEL software.

References

1) KLUEPFEL, D.; H. A. BAKER, G. PIATTONI, S. N. SEHGAL, A. SIDOROWICZ, K. SINGH & C. VÉZINA: Naphthyridinomycin, a new broad-spectrum antibiotic. J. Antibiotics 28: 497~502, 1975
2) ZMIJEWSKI, M. J., Jr. & M. GOEBEL: Cyanonaphthyridinomycin: A derivative of naphthyridinomycin. J. Antibiotics 35: 524~526, 1982
3) ZMIJEWSKI, M. J., Jr.; K. MILLER-HATCH & M. GOEBEL: Naphthyridinomycin, a DNA-reactive antibiotic. Antimicrob. Agents Chemother. 21: 787~793, 1982
4) ZMIJEWSKI, M. J., Jr.; M. GOEBEL & M. MIKOLAJCZAK: The in vitro interaction of naphthyridinomycin with DNA. Chem. Biol. Interact. 52: 361~375, 1985
5) BOYD, F. L.; S. F. CHEATHAM, W. REMERS, G. C. HILL & L. H. HURLEY: Characterization of the structure of the anthramycin-d(ATGCAT)$_2$ adduct by NMR and molecular modeling studies. Determination of the stereochemistry of the covalent linkage site, orientation in the minor groove of DNA, and effect on local DNA structure. J. Am. Chem. Soc. 112: 3279~3289, 1990

6) ITOH, J.; S. OMOTO, S. INOUYE, Y. KODAMA, T. HISAMATSU, T. NIIDA & Y. OGAWA: New semisynthetic antitumor antibiotics, SF-1739 HP and naphthocyanidine. J. Antibiotics 35: 642~644, 1982
7) ZMIJEWSKI, M. J., Jr. & M. J. MIKOLAJCZAK: Quinone modified derivatives of cyanonaphthyridinomycin. J. Antibiotics 36: 1767~1769, 1983
8) RAO, S. N.; U. C. SINGH & P. A. KOLLMAN: Molecular mechanics simulations on covalent complexes between anthramycin and DNA. J. Med. Chem. 29: 2484~2492, 1986
9) REMERS, W. A.; M. MABILIA & A. J. HOPFINGER: Conformation of complexes between pyrrolo[1,4]benzodiazepines and DNA. J. Med. Chem. 29: 2492~2503, 1986
10) ZAKRZEWSKA, K. & B. PULLMAN: Sequence specificity in binding of anthramycin to DNA. J. Biomol. Struct. Dyn. 1: 127~136, 1986
11) SYGUSCH, J.; F. BRISSE & S. HANESSIAN: Crystal structure of naphthyridinomycin. Acta Crys. B32: 1139~1142, 1976
12) ARORA, S. K. & M. B. COX: Molecular structure, conformation and interaction of cyanonaphthridinomycin. J. Biomol. Struct. Dyn. 3: 489~502, 1988
13) EVANS, D. A.; C. R. ILLIG & J. C. SADDLER: Stereoselective synthesis of (±)-cyanocycline. J. Am. Chem. Soc. 108: 2478~2479, 1986
14) WEINER, S. J.; P. A. KOLLMAN, D. A. CASE, U. C. SINGH, C. GHIO, G. ALAGONA, S. PROFETA, Jr. & P. WEINER: A new force field for molecular mechanical simulation of nucleic acids and proteins. J. Am. Chem. Soc. 106: 765~784, 1984
15) ALTONA, C. & M. SUNDARALINGAM: Conformational analysis of the sugar ring in nucleosides and nucleotides. A new description using the concept of pseudorotation. J. Am. Chem. Soc. 94: 8205~8212, 1972